

Reduced-order models for closed-loop wake control

Gilead Tadmor, Oliver Lehmann, Bernd R. Noack, Laurent Cordier, Joël Delville, Jean-Paul Bonnet and Marek Morzynski

Phil. Trans. R. Soc. A 2011 **369**, 1513-1524
doi: 10.1098/rsta.2010.0367

References

[This article cites 26 articles](#)

<http://rsta.royalsocietypublishing.org/content/369/1940/1513.full.html#ref-list-1>

Rapid response

[Respond to this article](#)

<http://rsta.royalsocietypublishing.org/letters/submit/roypta;369/1940/1513>

Subject collections

Articles on similar topics can be found in the following collections

[mechanical engineering](#) (171 articles)
[fluid mechanics](#) (173 articles)

Email alerting service

Receive free email alerts when new articles cite this article - sign up in the box at the top right-hand corner of the article or click [here](#)

To subscribe to *Phil. Trans. R. Soc. A* go to:
<http://rsta.royalsocietypublishing.org/subscriptions>

Reduced-order models for closed-loop wake control

BY GILEAD TADMOR^{1,*}, OLIVER LEHMANN¹, BERND R. NOACK²,
LAURENT CORDIER², JOËL DELVILLE², JEAN-PAUL BONNET²
AND MAREK MORZYŃSKI³

¹*Northeastern University, 440 Dana Building, 360 Huntington Avenue,
Boston, MA 02115-5000, USA*

²*Département Fluides, Institut Pprime, CNRS–Université de
Poitiers–ENSMA, UPR 3346, Thermique, Combustion, CEAT,
43 rue de l'aérodrome, 86036 Poitiers cedex, France*

³*Poznań University of Technology, Institute of Combustion Engines
and Transportation, ul. Piotrowo 3, 60-965 Poznań, Poland*

We review a strategy for low- and least-order Galerkin models suitable for the design of closed-loop stabilization of wakes. These low-order models are based on a fixed set of dominant coherent structures and tend to be incurably fragile owing to two challenges. Firstly, they miss the important stabilizing effects of interactions with the base flow and stochastic fluctuations. Secondly, their range of validity is restricted by ignoring mode deformations during natural and actuated transients. We address the first challenge by including shift mode(s) and nonlinear turbulence models. The resulting robust least-order model lives on an inertial manifold, which links slow variations in the base flow and coherent and stochastic fluctuation amplitudes. The second challenge, the deformation of coherent structures, is addressed by parameter-dependent modes, allowing smooth transitions between operating conditions. Now, the Galerkin model lives on a refined manifold incorporating mode deformations. Control design is a simple corollary of the distilled model structure. We illustrate the modelling path for actuated wake flows.

Keywords: reduced-order model; Galerkin models on manifolds; finite-time thermodynamics closure; control design; bluff-body wakes

1. Introduction

Flow control affects a remarkably broad scope and range of scales of engineered systems, from microfluidic devices to energy and transportation systems. Potential benefits can reach epic proportions. Closed-loop control is an enabler for higher efficiency over a broader operational envelope than passive and open-loop actuation and is essential for disturbance rejection.

*Author for correspondence (tadmor@ece.neu.edu).

One contribution of 15 to a Theme Issue ‘Flow-control approaches to drag reduction in aerodynamics: progress and prospects’.

As in other feedback control applications, modelling the physical mechanisms and control laws is a critical component of the design task. The tension between the complexity and nonlinearity of the general description by the Navier–Stokes equation (NSE), and the simplicity and robustness needs of design and implementation make the identification of reduced-order models (ROMs) of turbulent flows particularly challenging. Here, we describe a unifying framework to address three aspects of this challenge: modelling (i) the dissipative effects of neglected small scales, (ii) the stabilizing effects of ignored variations in the base flow, and (iii) the dynamic deformation of dominant flow structures. For reasons of clarity and simplicity, the two-dimensional flow in the wake of a circular cylinder at $Re = 100$ is used as the driving benchmark. The issues raised for model-based control in this simple example prevail in the transitional and turbulent regimes.

The paper is organized as follows. The triple decomposition perspective of Galerkin models is discussed in §2. This includes a review of least-order Galerkin models, from simple oscillatory to complex broadband frequency dynamics. In §3, we describe control-oriented wake models. In §4, we introduce the concept of Galerkin models on manifolds to account for dynamic mode deformations. The control view of mode deformation and of the proposed solution is discussed in §5. Our conclusion and perspective are summarized in §6.

2. The triple decomposition

Low-order Galerkin models are expressly designed to resolve few key coherent structures, and ignore large portions of the frequency and wavenumber spectrum. This objective is conceptualized in terms of the triple decomposition

$$\mathbf{u}(\mathbf{x}, t) = \underbrace{\mathbf{u}^B(\mathbf{x}, t)}_{\omega \ll \omega_c} + \underbrace{\mathbf{u}^C(\mathbf{x}, t)}_{\omega \sim \omega_c} + \underbrace{\mathbf{u}^S(\mathbf{x}, t)}_{\omega \gg \omega_c}. \quad (2.1)$$

Here, \mathbf{u}^B , \mathbf{u}^C and \mathbf{u}^S denote the slowly varying base flow, coherent structures and the remaining small scales, at oscillation frequencies $\omega \ll \omega_c$, $\omega \sim \omega_c$ and $\omega \gg \omega_c$, respectively. Concrete definitions of the dominant frequency ω_c and \mathbf{u}^B , \mathbf{u}^C and \mathbf{u}^S can be made in terms of the Fourier transform of the velocity field (see §4c). The purpose of the dynamical model is to resolve \mathbf{u}^C .

(a) Coherent structures at dominant frequencies

The Galerkin expansion is defined by a small set of space-dependent modes $\{\mathbf{u}_i\}_{i=1}^N$ and time coefficients $\{a_i(t)\}_{i=1}^N$,

$$\mathbf{u}(\mathbf{x}, t) \approx \mathbf{u}^B(\mathbf{x}) + \mathbf{u}^C(\mathbf{x}, t) \approx \mathbf{u}^B(\mathbf{x}) + \sum_{i=1}^N a_i(t) \mathbf{u}_i(\mathbf{x}). \quad (2.2)$$

For simplicity, we consider the simplest case in which the base flow is time-independent, e.g. the steady Navier–Stokes solution. A dynamical system,

governing the evolution of the time coefficients a_i , is ideally obtained by the projection of the (actuated) NSE on the subspace spanned by equation (2.2),

$$\dot{a}_i = c_i + \sum_{j=1}^N l_{ij} a_j + \sum_{j,k=1}^N q_{ijk} a_j a_k + f_i, \quad i = 1, \dots, N. \quad (2.3)$$

Here, c_i , l_{ij} and q_{ijk} are coefficients associated with the unactuated dynamics and f_i is the modal component of a forcing term.

The ingredients of a successful model are geared to guarantee both the quality of the kinematic approximation by equation (2.2) and the dynamic predictive power of equation (2.3). Mode-set selection is critical to both objectives. Empirical representations based on flow snapshots have the advantage of relatively easy computations and high resolution. The proper orthogonal decomposition (POD) minimizes the time-averaged residual of equation (2.2) [1]. Koopman, dynamic mode decomposition (DMD) [2,3] and temporal harmonic [4,5] modes extract individual frequencies. Balanced POD (BPOD) [6] extracts modes from dynamic, albeit linear, input–output considerations.

Kinematic resolution is all too often insufficient for a successful *dynamic* model. Some remedies include augmented expansion sets, revisited in §4, and calibration methods [7]. Here, we overview issues stemming from ignoring the dynamic roles of \mathbf{u}^B and \mathbf{u}^S , followed by least-order realizations, in §3.

(b) Base flow–low frequencies

The bilateral interaction between mean flow variations and unsteady fluctuations is essential to flow physics. Fluctuations affect the mean flow via the Reynolds stress, and mean flow variations affect the stability of fluctuations, with reduced production at higher fluctuation levels. ROM should therefore incorporate a mean-field representation as a key stabilizer. Lacking such a representation may lead to fragile models and inaccurate predictions, whereas adding a single *shift mode* to equation (2.2) may offer an ample solution [5,8]. An alternative for homogeneous coordinates is the computation of \mathbf{u}^B by the projection of the Reynolds equation on equation (2.2), feeding that base flow into the Galerkin system [9–11], thus adding a stabilizing cubic term. Both approaches effectively restrict the dynamics to an inertial manifold, whether in the NSE or in the Galerkin subspace.

(c) Small-scale fluctuations–high frequencies

Energy transfer from \mathbf{u}^C to \mathbf{u}^S is another essential stabilizing mechanism. Models range from a single eddy viscosity [9], modal eddy viscosities [12] to calibrated linear [13] and higher order terms. Noack *et al.* [14] explain frequent difficulties with calibrated linear terms by incompatibility with the nonlinear transfer mechanism and suggest a nonlinear finite time thermodynamics (FTT)-based closure, tested for simple oscillatory to broadband dynamics.

Additionally, \mathbf{u}^S may contribute to dynamically essential high-frequency fluctuations in equation (2.3). Meteorological and some fluid-dynamical models represent this effect by white noise. Improved representations employ random time series that mimic the spectral distributions of POD expansions of \mathbf{u}^S ,

whether measured or hypothesized *a priori*, e.g. from a modified von Kármán spectrum [15]. An alternative is to employ stochastic models that realize a postulated scaling law for the energy level λ_i of the i th POD mode. Examples are an observed $\lambda_i \propto i^{-11/9}$ scaling for the POD eigenvalues in inhomogeneous turbulent flows [16], and linking the frequency ω to the POD mode index $i: \omega \propto i^{-\beta}$. As in FTT models, these representations do not resolve phase relationships.

3. Least-order Galerkin models

(a) Mean-field and turbulence models: single-frequency dynamics

A least-order model, i.e. one that captures dominant fluctuations with the least state space dimension, may resolve (i) changes in \mathbf{u}^B between the steady solution \mathbf{u}_s and the attractor's mean, \mathbf{u}_0 , using a normalized *shift mode* $\mathbf{u}_\Delta \propto \mathbf{u}_0 - \mathbf{u}_s$, and approximating $\mathbf{u}^B = \mathbf{u}_s + a_\Delta \mathbf{u}_\Delta$, (ii) an oscillatory mode pair, in $\mathbf{u}^C = a_1 \mathbf{u}_1 + a_2 \mathbf{u}_2 \approx A_n(\cos(\phi)\mathbf{u}_1 + \sin(\phi)\mathbf{u}_2)$, and (iii) higher harmonics, aggregated in \mathbf{u}^S . The resulting triple decomposition is characterized by the natural oscillation amplitude, A_n , the frequency, $\omega = d\phi/dt$, and the shift-mode amplitude, a_Δ , and reads

$$\mathbf{u} = \underbrace{\mathbf{u}_s + a_\Delta \mathbf{u}_\Delta}_{\mathbf{u}^B} + \underbrace{a_1 \mathbf{u}_1 + a_2 \mathbf{u}_2}_{\mathbf{u}^C} + \underbrace{\mathbf{u}^S}_{\text{higher harmonics}}. \quad (3.1)$$

Following [8], the Galerkin system (2.3) is simplified to

$$\frac{d}{dt} a_1 = \sigma a_1 - \omega a_2, \quad (3.2a)$$

$$\frac{d}{dt} a_2 = \sigma a_2 + \omega a_1 \quad (3.2b)$$

$$\text{and} \quad \frac{d}{dt} a_\Delta = -\sigma_\Delta a_\Delta + c(a_1^2 + a_2^2), \quad (3.2c)$$

where $\sigma = \sigma_1 - \beta_\Delta^* a_\Delta - \beta_S^* A_n^2$ and $\omega = \omega_1 + \gamma_\Delta^* a_\Delta$. The Galerkin expansion (3.1) is a realization of the triple decomposition (2.1) for an oscillatory flow. The growth rate σ and frequency ω in the Galerkin system (3.2a) and (3.2b) are composed of three components. The first, with σ_1, ω_1 , describes the linear instability ($a_\Delta = 0$). The a_Δ -dependent terms $\beta_\Delta^* a_\Delta$ and $\gamma_\Delta^* a_\Delta$ characterize the effect of mean-field deformation. The third term, $\beta_S^* A_n^2$, represents the energy-transfer rate, from resolved to higher harmonics, slaving $\|\mathbf{u}^S\|$ to A_n^2 . This dynamical system has been derived from an FTT closure [17] incorporating mean-field theory (see [14] for details).

A centre-manifold-type approximation of the actuated system, i.e. slaving a_Δ to A_n^2 and adding a forcing term, yields a Landau equation for the amplitude A_n ,

$$\frac{dA_n}{dt} = \sigma_1 A_n - \beta_\Delta A_n^3 - \beta_S A_n^3 + f. \quad (3.3)$$

Here, $\sigma_1 A_n$, $-\beta_\Delta A_n^3$ and $-\beta_S A_n^3$ represent the instability of \mathbf{u}^C , and the stabilizing effects of low frequencies in \mathbf{u}^B and high frequencies in \mathbf{u}^S , respectively. The key observation is that a viable homogeneous model is impossible without

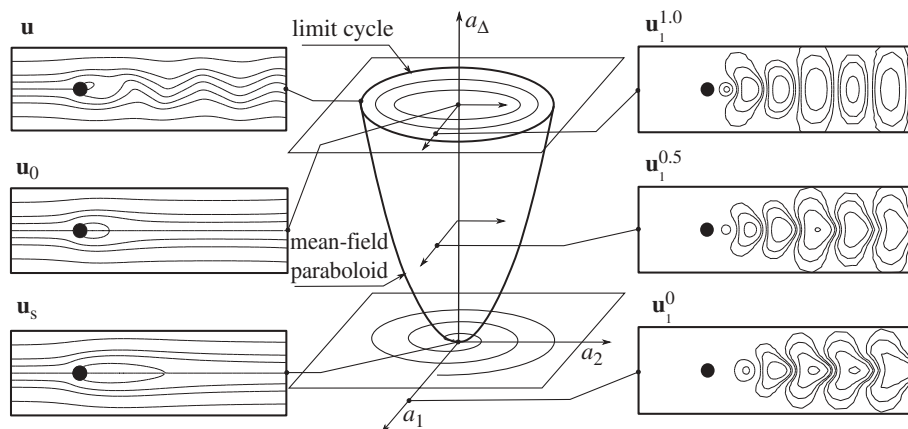


Figure 1. Principal sketch of the transient wake dynamics (for details see text).

the *nonlinear* stabilizing terms. Figure 1 illustrates the manifold $a_\Delta \propto A^2$ and the related flow states. It also illustrates mode deformations along transients, which we will discuss in §4. A properly designed oscillatory feedback (see §5) yields $f \propto -A$ in a stabilizing opposition control, akin to those employed in numerous wake and cavity control studies [18,19].

(b) *Mean-field and turbulence models: multiple frequencies dynamics*

Synchronizing control with state oscillations may become impractical, and design may use the stabilizing effect of high- or low-frequency actuation [20,21]. A least-order model in a two-frequency example contains three ingredients generalizing §3a: (i) a base flow $\mathbf{u}^B = \mathbf{u}_0^2 + a_\Delta \mathbf{u}_\Delta$, now defining $\mathbf{u}^\Delta \propto \mathbf{u}_0^a - \mathbf{u}_0^n$, connecting the natural and the actuated mean flows, \mathbf{u}_0^n and \mathbf{u}_0^a , (ii) a four-mode counterpart of the single frequency \mathbf{u}^C with the natural and actuated frequencies, ω_n and ω_a , and oscillation amplitudes A_n and A_a , and (iii) the high-frequency residual \mathbf{u}^S . The resulting coupled dynamics obey

$$\frac{dA_n}{dt} = \sigma_n A_n \quad \text{and} \quad \frac{dA_a}{dt} = \sigma_a A_a + B \cos(\phi - \phi_0). \quad (3.4)$$

Here, $\sigma_a < 0$ is the damping at ω_a , and, as in equation (3.3), $\sigma_n = \sigma_{n1} - \beta_{nn} A_n^2 - \beta_{na} A_a^2$. Unactuated, $A_a \equiv 0$ and equation (3.4) becomes equation (3.3). A mechanism we identified in wakes and high-lift configurations [21] is the reduced production of natural fluctuations, hence $\sigma_n < 0$ and the attenuation of A_n , once the mean field is modified by the Reynolds stress owing to actuated oscillations at large A_a . Again, a compelling case is made for the essential roles of nonlinear mean-field and turbulence representations, structurally rooted in the NSE.

(c) *Intermediate frequency band dynamics and richer mode sets*

Models based on few distinct frequencies and modes are feasible when operating conditions are narrowly defined. Model coefficients can then be calibrated, e.g. by Tikhonov methods [7]. The deforming effects of actuation and long transients on

leading flow structures, an issue we discuss in §4, require richer expansion sets. Computationally demanding robust design addresses uncertainty with ensemble-based methods [22]. Alternatively, an optimally representative POD database is created by sophisticated sampling of the control parameter space [23]. In a simpler scheme, considerable computational savings are also achievable when POD bases are derived from transients driven by an amply rich, frequency-varying excitation: a mere 40-mode expansion was used to determine the optimal control that minimizes the mean drag for a cylinder wake configuration [24]. This model covers 98 per cent of the total fluctuation kinetic energy (TKE) throughout the investigated regime.

(d) Broadband dynamics

Generally applicable model reduction methods are incapable in resolving the complex interplay of a large ensemble of nearly equally important modes. Successful examples invariantly focus on simpler dynamics in invariant subspaces. Examples include highly symmetric flows [1], and the *most observable decomposition* (MOD), optimizing the resolution of the control goal for turbulent jet noise [25]. Likewise, the BPOD [6] exploits (linear) input–output dynamics for relevant subspace identification. Otherwise, successful flow control relies on models and actuation that require only the slowly varying bulk statistical properties of the flow.

4. Galerkin models with deformable modes

(a) Evolving coherent structures, the need and modelling options

Figures 1 and 2 illustrate mode deformations over significant transients, and the resulting deteriorated model resolution, away from nominal conditions. Remedies include: (i) *augmented mode sets* derived from transients, multiple datasets (see figure 2), Navier–Stokes residuals and sensitivity analysis [26–28], (ii) *online adaptation* [29,30], and (iii) *pre-computed interpolated bases*, which is the topic of this section [31,32].

The rationale for adaptation, in (ii) or (iii), is the dimensional gap between local and global approximations: a persistent 95 per cent TKE transient resolution requires an 11-mode global basis. Figure 2 demonstrates the same resolution with only three deformable modes. This ratio worsens for wider operational envelopes.

(b) Mode deformation: the manifold embedding view

We use a measurable variable, $\alpha \in \mathcal{A}$, to reflect the slowly varying operating point, and use it to parametrize the base flow $\mathbf{u}^B = \mathbf{u}_0^\alpha$ and expansion modes $\{\mathbf{u}_i^\alpha\}_{i=1}^N$, at that point. In addition to state attributes (e.g. the TKE, estimated from sensor input), α may reflect exogenous effects, e.g. unsteady boundary conditions and actuation. The parametrized Galerkin expansion embeds the flow state in an *approximate inertial manifold* [33,34],

$$\mathbf{u}(\mathbf{x}, t) \approx \mathbf{u}_0^\alpha(\mathbf{x}, t) + \sum_{i=1}^N a_i(t) \mathbf{u}_i^\alpha(\mathbf{x}). \quad (4.1a)$$

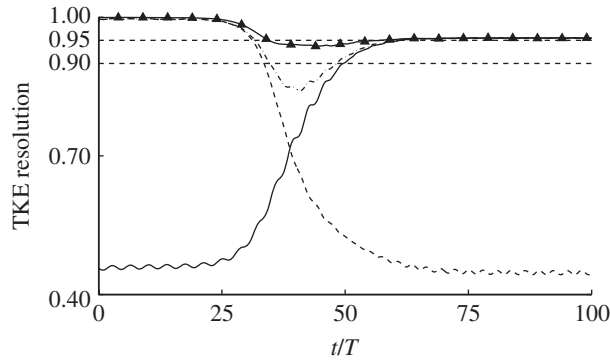


Figure 2. TKE resolution by several Galerkin expansions, during the cylinder wake's natural transient. The resolution is normalized with the instantaneous fluctuation energy. All approximations include the shift mode and two or four other oscillatory modes. One approximation (dashed line) uses the unstable eigenmodes of the NSE linearization at \mathbf{u}_s . An excellent early transient approximation is severely deteriorated towards the attractor. The reverse trend is observed for an expansion employing only the first two POD modes (solid line). A hybrid five-state model (dash-dot line) includes POD and stability modes, leading to significant improvement when compared with the previous expansions. Persistently the best resolution is obtained with a single, parametrized harmonic mode-pair (solid line with triangles) that deforms with changes in the operating point.

The Galerkin projection of the NSE now includes terms owing to modal time derivatives, $\partial_\alpha \mathbf{u}_i^\alpha d\alpha/dt$, $i = 0, \dots, N$, in equation (4.1a). This expands equation (2.3) to

$$\dot{a}_i = c_{0,i}^\alpha + \sum_{j=1}^N l_{0,ij}^\alpha a_j + \sum_{j,k=1}^N q_{0,ijk}^\alpha a_j a_k + \left(c_{1,i}^\alpha + \sum_{j=1}^N l_{1,ij}^\alpha a_j \right) \dot{\alpha} + f_i, \quad i = 1, \dots, N. \quad (4.1b)$$

With \mathbf{u}_i^α in the $L_2(\Omega)$ unit sphere, gradient orthogonality, $\partial_\alpha \mathbf{u}_k^\alpha \perp \mathbf{u}_k^\alpha$, can be used in an analytical computation of the deformation path, as an alternative to the empirical derivation suggested in §4c (see [35]). The $\dot{\alpha}$ -dependent global force field is a new representation of the impact of rapidly changing flow conditions, while remaining small during generic slower transients.

(c) Parametrization and harmonic modes

A method to derive expansion sets amenable to smooth, short-path parametrizations is a basic ingredient of the outlined framework. Linear (including geodesic) interpolation of POD modes [31,32] is a natural option. An effective variant for harmonically dominated flows is to compute equation (4.1a) as an α -dependent harmonic expansion (allowing incommensurate frequencies!), where the modes are evaluated as slowly varying, spatially distributed, temporal Fourier coefficients over a moving window $I(t) = [t - \frac{1}{2}T, t + \frac{1}{2}T]$ [4,5]. The instantaneous frequency is estimated, e.g. by analysing velocity trajectories over a small subdomain, $\Omega_f \subset \Omega$, where the sought harmonic is known to be prominent. This approach implicitly resolves the otherwise delicate issue of optimal alignment of \mathbf{u}_k^α for varying α . An efficient parametrization of each $\{\mathbf{u}_k^\alpha\}_{\alpha \in \mathcal{A}}$

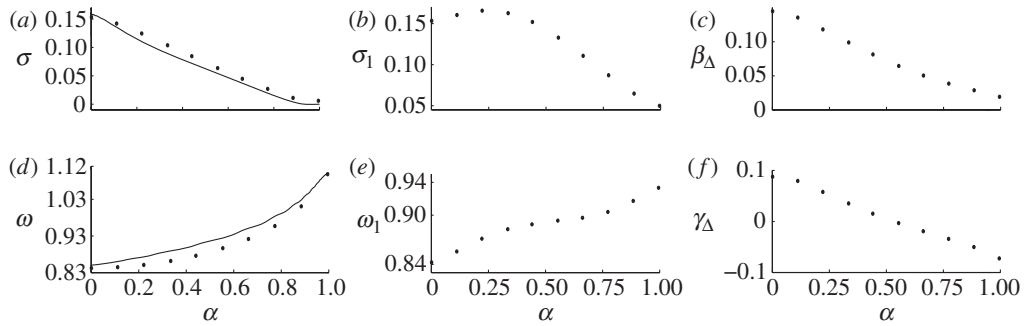


Figure 3. Parametrized Galerkin model evaluation. (*a–c*) Transient values of the growth rate $\sigma = (dA_n/dt)/A_n$ (*a*), (solid line) are in good agreement with values of $\sigma = \sigma_1 - \beta_\Delta a_\Delta$, as obtained by the Galerkin projection over the parametrized modes at the respective values of α . (*b,c*) The corresponding Galerkin projection values of σ_1 and β_Δ . (*d–f*) Transient values of the oscillation frequency (*d*), (solid line) are in good agreement with the Galerkin model predictions of $\omega = \omega_1 - \gamma_\Delta a_\Delta$. (*e,f*) The Galerkin projection values of ω_1 and γ_Δ . Operating points are parametrized by $\alpha := A_n^{1.5}/\max(A_n^{1.5})$.

is achieved by POD analysis, not unlike the double POD (DPOD) method [36]. The significant departure from augmented mode set approaches, like the DPOD, is that the α -parametrization is purely *kinematic*, adding no *dynamic* state. This organic outgrowth of the frequency-centred triple decomposition perspective was instrumental in unveiling the Navier–Stokes foundations of the generalized mean-field model in Luchtenburg *et al.* [21] and Tadmor *et al.* [5].

Figure 3 illustrates the dynamic quality of the parametrized model (4.1), where $\alpha := A_n^{1.5}/\max(A_n^{1.5})$ parametrizes the operating point.¹ The figure compares evaluations of the instantaneous exponential growth rate, $\sigma = (dA_n/dt)/A_n$, and of the shedding frequency, ω , from the transient Navier–Stokes state with $\sigma_1 - \beta_\Delta a_\Delta$ and $\omega_1 - \gamma_\Delta a_\Delta$ from Galerkin projections on the parametrized least-order expansion (i.e. \mathbf{u}_i^α , $i=0,1,2$, spanning \mathbf{u}^C and \mathbf{u}^B), at 10 values of α (dots). The remarkable match with the Navier–Stokes simulation is a testimony to the validity and value of a parametrized least-order model. A small residual reflects the need for a turbulence model and the effects of the phase lag in the transient a_Δ . The base flow and modes are parametrized by very smooth interpolation of four velocity fields for $\mathbf{u}_\Delta^\alpha := \mathbf{u}_0^\alpha - \mathbf{u}_s$, and three fields each, for \mathbf{u}_i , $i=1,2$ (not shown).

5. Feedback wake stabilization

The cylinder wake flow, actuated by a local, oscillatory body force, is a simple illustration. The body force is modulated by the control command $b(t) = B \cos(\phi(t) + \theta)$, with slowly varying B and θ , defining the control command. The forcing term in the amplitude equation (3.3) then includes a negligible second harmonic component, and the slowly varying $f_{dc} = gB \cos(\theta)$, where g is a gain [18]. Critical observations on an effective feedback actuation are derived from this formulation: (i) the values of θ and of the state oscillation phase, ϕ ,

¹The TKE $A_n^2/2$ or A_n would work as well. The 1.5 power is used merely for plot clarity.

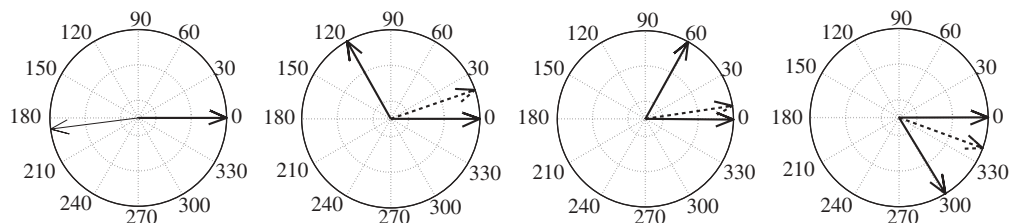


Figure 4. The oscillation phase shift of the optimally stabilizing actuation (dashed arrow) and of a sensor signal (solid arrow) are defined relative to the phase of the oscillatory flow, which is always represented by the bold arrow pointing at 0° . The four plots represent four states between the steady solution \mathbf{u}_s (left) and the natural attractor (right). The actuation phase shift is 0° in the left plot. The optimal phase shift between the oscillatory actuation command and sensor signal varies from over $+180^\circ$ (left) to about -40° (right), illustrating the need for continuous model adjustment for successful stabilization.

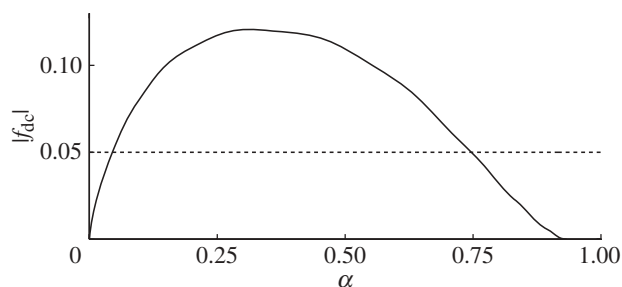


Figure 5. The critical $|f_{dc}|$ -level necessary to balance the natural destabilizing force (solid line). The same actuation level (horizontal dashed line) matches the critical level at two points: a dynamically stable point (right), at higher oscillation amplitude, and an unstable point, at lower oscillation amplitude (left).

need to be accurately evaluated to determine a stabilizing actuation, i.e. $f_{dc} < 0$; an incorrect evaluation may lead to a destabilizing $f_{dc} > 0$; (ii) likewise, a realistic sensor-based feedback must correctly assess the phase shift between sensor signal oscillations and the oscillatory state; (iii) B must be sufficiently large to make $(\sigma_1 - \beta_\Delta A^2 - \beta_S A^2)A + f_{dc} < 0$, but not too large, to avoid driving the flow away from the model's validity envelope.

Concerning (i) and (ii), figure 4 shows the changes in the required phase shift between sensor and actuator oscillations, as the flow is driven from the attractor towards \mathbf{u}_s . These changes cannot be predicted by a model using a single, fixed mode set, leading to poor performance [18]. It is dramatically improved by simple, parametrized model-based look-up table feedback [37]. In Noack *et al.* [14], we discuss the instability of phase observers, as A_n subsides.

Concerning (iii), figure 5 depicts the critical amplitude of f_{dc} , as read from the α -dependent cubic polynomial condition $(\sigma_1 - \beta_\Delta A^2 - \beta_S A^2)A + f_{dc} = 0$. The dashed horizontal line illustrates the fact that the same actuation amplitude fits two operating points, where it crosses the critical amplitude curve. The right crossing is at a dynamically stable point, whereas the left one, reflecting a lower

oscillation amplitude, is unstable, revealing an inherent performance limitation and explaining observed transitions to closed-loop limit cycles when A_n , hence α , crosses the critical value where $|f_{dc}|$ peaks.

6. Concluding remarks

We reviewed intrinsic challenges to robust low- and least-order models for wake stabilization, and outlined a unified framework that identifies and aims to remove the root causes of these stumbling blocks. Concepts of state partitioning by temporal frequencies and spatial length scales permeate the discussion: the triple decomposition frames the need to account for—rather than resolve—the dynamic impact of neglected small and large scales. Finite-time thermodynamics and generalized mean-field theory, derived from first principles, provide the tools to address these issues. Simple and robust, low-order manifold embedding resolves the deformation of modelled coherent structures, as flow conditions change. This is an attractive alternative to the complexity and potential numerical sensitivity of using the entire geometric aggregate of the local models, throughout the operational envelope. Here, too, the role of harmonic expansions is central. Wake flow stabilization is used to illustrate the criticality of the parametrized model, as well as the power of the simplest, least-order model, when endowed with an ample representation of neglected length scales. Follow-up and complementary details in Noack *et al.* [14] concern concrete representation formalisms for boundary forcing (by disturbance of actuation), including unsteady acceleration and velocity fields across the boundary and forced and aeroelastic wall deformation.

References

- 1 Holmes, P., Lumley, J. L. & Berkooz, G. 1998 *Turbulence, coherent structures, dynamical systems and symmetry*. Cambridge, UK: Cambridge University Press.
- 2 Rowley, C. W., Mezić, I., Bagheri, S., Schlatter, P. & Henningson, D. S. 2009 Spectral analysis of nonlinear flows. *J. Fluid Mech.* **645**, 115–127. (doi:10.1017/S0022112009992059)
- 3 Schmid, P. J. 2010 Dynamic mode decomposition for numerical and experimental data. *J. Fluid Mech.* **656**, 5–28. (doi:10.1017/S0022112010001217)
- 4 Tadmor, G., Bisseck, D., Noack, B. R., Morzyński, M., Colonius, T. & Taira, K. 2008 Temporal-harmonic specific POD mode extraction. In *Proc. 4th Flow Control Conf./38th AIAA Fluid Dynamics Conf. and Exhibit*, Seattle, WA, 23–26 June 2008. AIAA Paper 2008–4190. Reston, VA: American Institute for Aeronautics & Astronautics.
- 5 Tadmor, G., Lehmann, O., Noack, B. R. & Morzyński, M. 2010 Mean field representation of the natural and actuated cylinder wake. *Phys. Fluids* **22**, 034102. See <http://link.aip.org/link/?PHF/22/034102/1>. (doi:10.1063/1.3298960)
- 6 Rowley, C. W. 2005 Model reduction for fluids using balanced proper orthogonal decomposition. *Int. J. Bifurcat. Chaos* **15**, 997–1013. (doi:10.1142/S0218127405012429)
- 7 Cordier, L., Abou El Majd, B. & Favier, J. 2010 Calibration of POD reduced-order models using Tikhonov regularization. *Int. J. Numer. Meth. Fluids* **63**, 269–296. (doi:10.1002/fl.2074)
- 8 Noack, B. R., Afanasiev, K., Morzyński, M., Tadmor, G. & Thiele, F. 2003 A hierarchy of low-dimensional models for the transient and post-transient cylinder wake. *J. Fluid Mech.* **497**, 335–363. (doi:10.1017/S0022112003006694)
- 9 Aubry, N., Holmes, P., Lumley, J. L. & Stone, E. 1988 The dynamics of coherent structures in the wall region of a turbulent boundary layer. *J. Fluid Mech.* **192**, 115–173. (doi:10.1017/S0022112088001818)

- 10 Ukeiley, L., Cordier, L., Manceau, R., Delville, J., Bonnet, J. P. & Glauser, M. 2001 Examination of large-scale structures in a turbulent plane mixing layer. Part 2. Dynamical systems model. *J. Fluid Mech.* **441**, 61–108. (doi:10.1017/S0022112001004803)
- 11 Podvin, B. 2009 A proper-orthogonal-decomposition based for the wall layer of a turbulent channel flow. *Phys. Fluids* **21**, 015111. (doi:10.1063/1.3068759)
- 12 Rempfer, D. & Fasel, F. H. 1994 Dynamics of three-dimensional coherent structures in a flat-plate boundary-layer. *J. Fluid Mech.* **275**, 257–283. (doi:10.1017/S0022112094002351)
- 13 Galletti, G., Bruneau, C. H., Zannetti, L. & Iollo, A. 2004 Low-order modelling of laminar flow regimes past a confined square cylinder. *J. Fluid Mech.* **503**, 161–170. (doi:10.1017/S0022112004007906)
- 14 Noack, B. R., Morzyński, M. & Tadmor, G. (eds) 2010 *Reduced-order modelling for flow control*. Berlin, Germany: Springer.
- 15 Perret, L., Delville, J., Manceau, R. & Bonnet, J.-P. 2008 Turbulent inflow conditions for large-eddy simulation based on low-order empirical model. *Phys. Fluids* **20**, 075107. See <http://link.aip.org/link/?PHF/20/075107/1> (doi:10.1063/1.2957019)
- 16 Knight, B. & Sirovich, L. 1990 Kolmogorov inertial range for inhomogeneous turbulent flows. *Phys. Rev. Lett.* **65**, 1356–1359. (doi:10.1103/PhysRevLett.65.1356)
- 17 Noack, B. R., Schlegel, M., Ahlborn, B., Mutschke, G., Morzyński, M., Comte, P. & Tadmor, G. 2008 A finite-time thermodynamics of unsteady fluid flows. *J. Non-Equilib. Thermodyn.* **33**, 103–148. (doi:10.1515/JNETDY.2008.016)
- 18 Gerhard, J., Pastoor, M., King, R., Noack, B. R., Dillmann, A., Morzyński, M. & Tadmor, G. 2003 Model-based control of vortex shedding using low-dimensional Galerkin models. In *Proc. 33rd AIAA Fluids Conf. and Exhibit, Orlando, FL, 23–26 June 2003*. Paper 2003–4262. Reston, VA: American Institute for Aeronautics & Astronautics.
- 19 Samimy, M., Debiasi, M., Caraballo, E., Serrani, A., Yuan, X., Little, J. & Myatt, J.-H. 2007 Feedback control of subsonic cavity flows using reduced-order models. *J. Fluid Mech.* **579**, 315–346. (doi:10.1017/S0022112007005204)
- 20 Pastoor, M., Henning, L., Noack, B. R., King, R. & Tadmor, G. 2008 Feedback shear layer control for bluff body drag reduction. *J. Fluid Mech.* **608**, 161–196. (doi:10.1017/S0022112008002073)
- 21 Luchtenburg, D. M., Günter, B., Noack, B. R., King, R. & Tadmor, G. 2009 A generalized mean-field model of the natural and actuated flows around a high-lift configuration. *J. Fluid Mech.* **623**, 283–316. (doi:10.1017/S0022112008004965)
- 22 Mathelin, L. & Le Maitre, O. 2009 Robust control of uncertain cylinder wake flows based on robust reduced order models. *Comp. Fluids* **38**, 1168–1182. (doi:10.1016/j.compfluid.2008.11.009)
- 23 Burkardt, J., Gunzburger, M. D. & Lee, H.-C. 2004 Centroidal Voronoi tessellation-based reduced-order modeling of complex systems. Technical report, Florida State University, USA.
- 24 Bergmann, M., Cordier, L. & Brancher, J.-P. 2005 Optimal rotary control of the cylinder wake using proper orthogonal decomposition reduced order model. *Phys. Fluids* **17**, 097101. (doi:10.1063/1.2033624)
- 25 Schlegel, M., Noack, B. R., Comte, P., Kolomenskiy, D., Schneider, K., Farge, M., Scouten, J., Luchtenburg, D. M. & Tadmor, G. 2009 Reduced-order modelling of turbulent jets for noise control. In *Numerical simulation of turbulent flows and noise generation: results of the DFG/CNRS research groups FOR 507 and FOR 508*. Notes on Numerical Fluid Mechanics and Multidisciplinary Design (NNFM), pp. 3–27. Berlin, Germany: Springer.
- 26 Jørgensen, B. H., Sørensen, J. N. & Brøns, M. 2003 Low-dimensional modeling of a driven cavity flow with two free parameters. *Theor. Comput. Fluid Dyn.* **16**, 299–317. (doi:10.1007/s00162-002-0082-9)
- 27 Hay, A., Borggaard, J. & Pelletier, D. 2009 Local improvements to reduced-order models using sensitivity analysis of the proper orthogonal decomposition. *J. Fluid Mech.* **629**, 41–72. (doi:10.1017/S0022112009006363)
- 28 Bergmann, M., Bruneau, C.-H. & Iollo, A. 2009 Enablers for robust POD models. *J. Comp. Phys.* **228**, 516–538. (doi:10.1016/j.jcp.2008.09.024)

- 29 Ravindran, S. S. 2000 Reduced-order adaptive controllers for fluid flows using POD. *J. Sci. Comput.* **15**, 457–478. (doi:10.1023/A:1011184714898)
- 30 Bergmann, M. & Cordier, L. 2008 Optimal control of the cylinder wake in the laminar regime by trust–region methods and POD reduced order models. *J. Comp. Phys.* **227**, 7813–7840. (doi:10.1016/j.jcp.2008.04.034)
- 31 Morzyński, M., Stankiewicz, W., Noack, B. R., King, R., Thiele, F. & Tadmor, G. 2007 Continuous mode interpolation for control-oriented models of fluid flow. In *Proc. Active flow control, Berlin, Germany, 27–29 September 2006*. Notes on Numerical Fluid Mechanics and Multidisciplinary Design, vol. 95 (ed. R. King), pp. 260–278. Berlin, Germany: Springer.
- 32 Amsallem, D. & Farhat, C. 2008 Interpolation method for adapting reduced-order models and application to aeroelasticity. *AIAA J.* **46**, 1803–1813. (doi:10.2514/1.35374)
- 33 Constantin, P., Foias, C., Nicolaenko, B. & Temam, R. 1989 *Integral manifolds and inertial manifolds for dissipative partial differential equations*. Berlin, Germany: Springer.
- 34 Gorban, A. N., Kazantzis, N. K., Kevrekidis, I. G., Öttinger, H. C. & Theodoropoulos, C. (eds) 2006 *Model reduction and coarse-graining approaches for multiscale phenomena*. Berlin, Germany: Springer.
- 35 Sapsis, T. P. & Lermusiaux, P. F. J. 2009 Dynamically orthogonal field equations for continuous stochastic dynamical system. *Phys. D* **238**, 2347–2360. (doi:10.1016/j.physd.2009.09.017)
- 36 Siegel, S. G., Seidel, J., Fagley, C., Luchtenburg, D. M., Cohen, K. & McLaughlin, T. 2008 Low dimensional modelling of a transient cylinder wake using double proper orthogonal decomposition. *J. Fluid Mech.* **610**, 1–42. (doi:10.1017/S0022112008002115)
- 37 Lehmann, O., Luchtenburg, M., Noack, B. R., King, R., Morzyński, M. & Tadmor, G. 2005 Wake stabilization using POD Galerkin models with interpolated modes. In *Proc. 44th IEEE Conf. on Decision and Control and European Control Conf. ECC, Seville, Spain, 12–15 December 2005*. Invited Paper MoA15.2. Piscataway, NJ: IEEE.